Novel neutron resonance mode in $d_{x^2-y^2}$-wave superconductors

I. Eremin,[1,*] D. K. Morr,[1,2] A. V. Chubukov,[3] K. H. Bennemann,[1] and M. R. Norman[4]

[1]*Institut für Theoretische Physik, Freie Universität Berlin, D-14195, Berlin, Germany*
[2]*Department of Physics, University of Illinois at Chicago, Chicago, Illinois 60607, USA*
[3]*Department of Physics, University of Wisconsin, Madison, Wisconsin 53706, USA*
[4]*Materials Science Division, Argonne National Laboratory, Argonne, Illinois 60439, USA*

(Received 8 September 2004; published 14 April 2005)

We show that a new resonant magnetic excitation at incommensurate momenta, observed recently by inelastic neutron scattering experiments on $YBa_2Cu_3O_{6.85}$ and $YBa_2Cu_3O_{6.6}$, is a *spin exciton*. Its location in the Brillouin zone and its frequency are determined by the momentum dependence of the particle-hole continuum. We identify several features that distinguish this novel mode from the previous resonance mode observed near $\mathbf{Q} = (\pi, \pi)$.

DOI: 10.1103/PhysRevLett.94.147001 PACS numbers: 74.25.Ha, 71.10.Ca, 74.20.Fg, 74.72.Bk

While it seems established that the resonance peak is a universal feature of the high-temperature superconductors [1–3], its origin, its role in pairing, and the effects arising from its interactions with electrons are still intensively debated [4]. The peak's intensity is the highest at $\mathbf{Q} = (\pi, \pi)$ and in $YBa_2Cu_3O_{6+x}$ (YBCO), where it was studied in great detail, its frequency $\Omega_{\rm res}(\mathbf{Q})$ follows the same doping dependence as T_c, with $\Omega_{\rm res}(\mathbf{Q}) \approx 41$ meV near optimal doping. As one moves away from $\mathbf{Q}$, the peak disperses downwards and its intensity decreases rapidly, vanishing around $\mathbf{Q}_0 = (0.8\pi, 0.8\pi)$. The doping dependence of $\Omega_{\rm res}(\mathbf{Q})$, the downward dispersion of the resonance, and the fact that $\mathbf{Q}_0$ coincides with the distance between nodal points on the Fermi surface are consistent with the theoretical idea that the resonance peak is a particle-hole bound state below the spin gap (a spin exciton) [5]. (For a review of other scenarios, see Ref. [6].)

Recent inelastic neutron scattering (INS) experiments in the superconducting (SC) state of YBCO [7–9] detected a new resonant magnetic excitation at incommensurate momenta, but at frequencies *larger* than $\Omega_{\rm res}(\mathbf{Q})$. It was suggested [7] that this new resonance is a particle-hole bound state which forms an upward dispersion originating at $\mathbf{Q}$. (See Fig. 4 in Ref. [7].)

In this Letter, we show that at least near optimal doping, the new resonance mode can be viewed as a spin exciton. This agrees with the explanation given in Ref. [7]. However, we demonstrate that the new exciton does *not* form an upward dispersing branch originating at $\mathbf{Q}$. Instead, it appears only at momenta less than $\mathbf{Q}_0$, and is separated from the ''old'' resonance by a region near $\mathbf{Q}_0$ in which no resonance exists (the ''silent band'' of Ref. [7]). We identify several qualitative features that distinguish this new resonance (the Q^* mode) from the old one (the Q mode). In particular, we show that (i) the Q and Q^* modes are due to direct and umklapp scattering, respectively, and (ii) the intensity of the Q^* mode is largest along $\eta(\pi, \pi)$, while the intensity of the Q mode is largest along $(\pi, \eta\pi)$ and $(\eta\pi, \pi)$.

We begin by presenting our numerical results for the new Q^* mode. Its emergence can be understood within a random phase approximation (RPA) approach for which the spin susceptibility is given by [10]

$$\chi(\mathbf{q}, \omega) = \frac{\chi_0(\mathbf{q}, \omega)}{1 - g(\mathbf{q})\chi_0(\mathbf{q}, \omega)}, \tag{1}$$

where $g(\mathbf{q})$ is the fermionic four-point vertex, and $\chi_0(\mathbf{q}, \omega)$ is the free-fermion susceptibility, which in the SC state is given by the sum of two single bubble diagrams consisting of either normal or anomalous Green's functions [5]. For our numerical calculation of $\chi_0(\mathbf{q}, \omega)$, we used a SC gap with $d_{x^2-y^2}$ symmetry and a normal state tight binding dispersion

$$\epsilon_{\mathbf{k}} = -2t(\cos k_x + \cos k_y) - 4t' \cos k_x \cos k_y - \mu \tag{2}$$

with $t = 250$ meV, $t'/t = -0.4$, and $\mu/t = -1.083$ [11]. The Fermi surface (FS) obtained from Eq. (2) is shown in Fig. 3(a). It describes well the FS measured by photoemission experiments on $Bi_2Sr_2CaCu_2O_{8+\delta}$ [12].

Our main results are presented in Figs. 1 and 2, in which we plot $\mathrm{Im}\chi(\mathbf{q}, \omega)$, obtained from a numerical evaluation of Eq. (1), along $\mathbf{q} = \eta(\pi, \pi)$ in the SC state. The intensity plot of $\mathrm{Im}\chi(\mathbf{q}, \omega)$ shown in Fig. 1 possesses the salient features observed in the INS experiments. First, the Q mode (indicated by a red arrow). Second, the Q^* mode (indicated by a yellow arrow) is located at frequencies larger than the frequency of the Q mode at (π, π), and is confined to a small region of momentum space near $\mathbf{Q}_0$. Third, there exists a region in momentum space around $\mathbf{Q}_0$ which separates the Q mode from the Q^* mode (the silent band of Ref. [7]). As $\mathbf{Q}_0$ is approached from (π, π), the Q mode frequency, $\Omega_{\rm res}(\mathbf{q})$, as well as its intensity, rapidly decreases. In Fig. 2 we present $\mathrm{Im}\chi$ along $\mathbf{q} = \eta(\pi, \pi)$ for several frequencies. We clearly see that the two modes are separated in momentum and frequency space. The shaded area in Fig. 2 represents the silent band, in which $\mathrm{Im}\chi$ is strongly reduced from its resonance values. We also find that the position of the Q^* mode is almost frequency independent, with a maximum intensity at $\omega \approx 54$ meV,

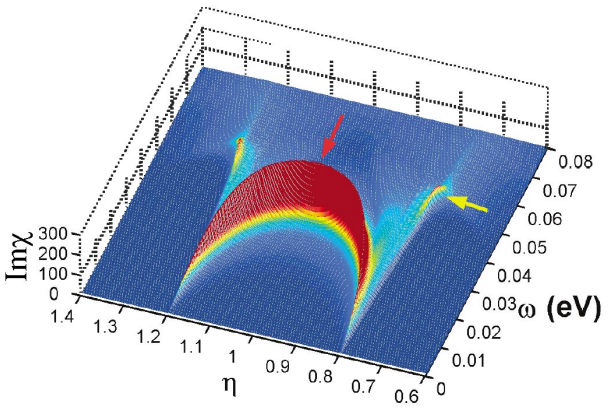

FIG. 1 (color). RPA results for magnetic excitations in a $d_{x^2-y^2}$ superconductor. Imχ obtained from Eq. (1) as a function of momentum [along $\mathbf{q} = \eta(\pi, \pi)$] and frequency in the SC state. We use $\Delta_{\mathbf{k}} = \Delta_0(\cos k_x - \cos k_y)/2$ with $\Delta_0 = 42$ meV, and $g(\mathbf{q})$ weakly peaked at (π, π): $g(\mathbf{q}) = g_0[1 - 0.1(\cos q_x + \cos q_y)]$ with $g_0 = 0.572$ eV, in order to reproduce the correct energy position of the Q^* mode near $0.8(\pi, \pi)$ and the Q mode at (π, π).

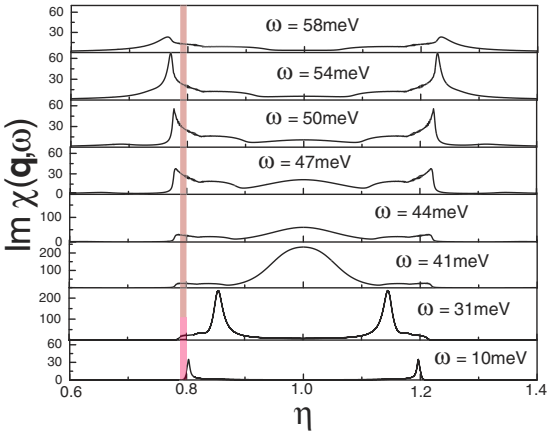

FIG. 2 (color online). Im$\chi(\mathbf{q}, \omega)$ along $\mathbf{q} = \eta(\pi, \pi)$ for several frequencies. The position of the silent band is indicated by the shaded area. The Q mode disperses downwards from $\omega \approx 41$ meV as η deviates from 1 and disappears at $\eta = 0.8$. At smaller η, the Q^* mode emerges with a maximum intensity at $\omega \approx 54$ meV.

in agreement with the experimental observations of Ref. [7].

We next discuss the physical origin of the new resonance. We recall that the (π, π) spin exciton emerges due to a feedback effect of the SC gap on χ_0. To see this, we split $\chi_0(\mathbf{Q}, \Omega)$ into a static and a dynamic part: $\chi_0(\mathbf{Q}, \Omega) = \chi_0(\mathbf{Q}, 0) + \Delta\chi_0(\mathbf{Q}, \Omega)$. In the paramagnetic state, $1 - g(\mathbf{Q})\chi_0(\mathbf{Q}, 0) = \xi_{\mathbf{Q}}^{-2} > 0$. The dynamic part $\Delta\chi_0(\mathbf{Q}, \Omega)$ at $T = 0$ is given by [13]

$$\Delta\chi_0(\mathbf{Q}, \Omega) = -i\frac{\gamma_{\mathbf{Q}}^{NS}}{16}\sum_{\{\mathbf{k},\mathbf{k}'\}} \times \int_{-\infty}^{\infty} d\omega\left(1 - \frac{\omega_+\omega_- + \Delta_{\mathbf{k}}\Delta_{\mathbf{k}'}}{\sqrt{\omega_+^2 - \Delta_{\mathbf{k}}^2}\sqrt{\omega_-^2 - \Delta_{\mathbf{k}'}^2}}\right) \quad (3)$$

where $\omega_\pm = \omega \pm \Omega/2$, and the summation runs over all pairs of FS points $\mathbf{k}$ and $\mathbf{k}'$ separated by $\mathbf{Q}$ (hot spots). There are eight scattering processes from $\mathbf{k}$ to $\mathbf{k}'$ in the first zone. The momenta $\mathbf{k}$ involved are those in which the boundary of the magnetic zone (defined by $\cos k_x = -\cos k_y$) crosses the FS. Two of these scattering processes are direct with $\mathbf{k} - \mathbf{k}' = \mathbf{Q}$, two involve umklapp scattering with $\mathbf{k} - \mathbf{k}' = \mathbf{Q} - (2\pi, 2\pi)$, and four involve umklapp scattering with $\mathbf{k} - \mathbf{k}' = \mathbf{Q} - (2\pi, 0)$ and $\mathbf{k} - \mathbf{k}' = \mathbf{Q} - (0, 2\pi)$. A pair of FS points that are connected by direct scattering via $\mathbf{Q}$ is shown in Fig. 3(a) ($\mathbf{Q}$ is represented by a dashed arrow).

In the normal state, all eight processes equally contribute to $\Delta\chi_0(\mathbf{Q}, \Omega)$, and one obtains from Eq. (3) $\Delta\chi_0(\mathbf{Q}, \Omega) = -i\gamma_{\mathbf{Q}}^{NS}\Omega$ which identifies $\gamma_{\mathbf{Q}}^{NS}$ with the Landau damping rate [14]. In the SC state, $\Delta\chi_0$ becomes a complex function. According to Eq. (3), its imaginary part vanishes below a critical frequency $\Omega_c(\mathbf{Q}) = |\Delta_{\mathbf{k}}| + |\Delta_{\mathbf{k}'}|$, which is the same for all eight scattering channels. The $d_{x^2-y^2}$ symmetry of the SC gap implies $\Delta_{\mathbf{k}} = -\Delta_{\mathbf{k}'}$, resulting in a discontinuous jump of Imχ_0 at $\Omega_c(\mathbf{Q})$ from zero to $\pi\gamma_{\mathbf{Q}}^{NS}|\Delta_{\mathbf{k}}|$ [5]. Simultaneously, Re$\Delta\chi_0(\mathbf{Q}, \Omega) > 0$ is nonzero, diverges logarithmically at $\Omega_c(\mathbf{Q})$, and scales as Ω^2 at small frequencies. Re$\Delta\chi_0$ therefore varies between 0 at $\Omega = 0$ and ∞ at $\Omega = \Omega_c$. Since $\xi_{\mathbf{Q}}^{-2} > 0$, one finds that for any positive $g_{\mathbf{Q}}$, $\chi(\mathbf{Q}, \Omega)$ [Eq. (1)] acquires a pole below the particle-hole (p-h) continuum, at a frequency $\Omega_{\text{res}} < \Omega_c(\mathbf{Q})$, at which Re$\Delta\chi_0(\mathbf{Q}, \Omega_{\text{res}}) = \xi_{\mathbf{Q}}^{-2}/g_{\mathbf{Q}}$ and Im$\Delta\chi_0(\mathbf{Q}, \Omega_{\text{res}}) = 0$.

For $\mathbf{q} \neq \mathbf{Q}$, the degeneracy of the scattering channels is lifted. In particular, for $\mathbf{q} = \eta(\pi, \pi)$, one now has three different critical frequencies, $\Omega_c^{(i)}(\mathbf{q})$ $(i = 1, 2, 3)$ [5,15,16]. $\Omega_c^{(1)}$ is the critical frequency associated with direct scattering, $\Omega_c^{(2)}$ with umklapp scattering involving $\mathbf{q} - (2\pi, 0)$ and $\mathbf{q} - (0, 2\pi)$, and $\Omega_c^{(3)}$ with umklapp scattering by $\mathbf{q} - (2\pi, 2\pi)$. The scattering momenta for $\mathbf{q}$ close to $\mathbf{Q}_0$ are shown in Fig. 3(a), $\Omega_c^{(i)}(\mathbf{q})$ are presented

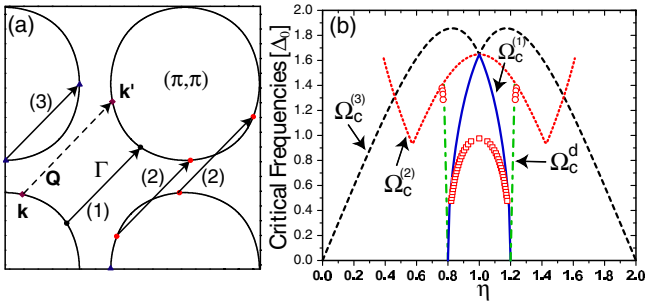

FIG. 3 (color online). (a) FS of Eq. (2) and magnetic scattering vectors. (b) Momentum dependence of the critical frequencies $\Omega_c^{(i)}$ $(i = 1, 2, 3)$ and the direct gap Ω_c^d along $\mathbf{q} = \eta(\pi, \pi)$; see text. The open squares (circles) represent the position of the $Q(Q^*)$ resonance.

in Fig. 3(b), and the behavior of $\mathrm{Im}\Delta\chi_0(\mathbf{q}, \Omega)$ is illustrated in Fig. 4(b). For all of these scattering processes, $\Delta_{\mathbf{k}}$ and $\Delta_{\mathbf{k}'}$ have opposite signs. As a result, $\mathrm{Im}\Delta\chi_0$ exhibits three discontinuous jumps at $\Omega_c^{(i)}(\mathbf{q})$, and $\mathrm{Re}\Delta\chi_0$ diverges logarithmically at $\Omega_c^{(i)}(\mathbf{q})$ [5]. However, $\mathrm{Im}\Delta\chi_0$ is zero only below the smallest $\Omega_c^{(i)}(\mathbf{q})$, and hence a true resonance is only possible below the smallest critical frequency [see Fig. 4(b)].

It follows from Fig. 3(b) that for $0.8 < \eta < 1.2$, the smallest critical frequency, $\Omega_c^{(1)}$, corresponds to direct (i.e., nonumklapp) scattering. $\Omega_c^{(1)}$ decreases away from $\eta = 1$ and eventually vanishes at $\eta = 0.8$, when direct scattering occurs between nodal points at the Fermi surface [5]. Since the exciton is located below $\Omega_c^{(1)}$, its frequency also decreases and vanishes at $\eta = 0.8$. Moreover, upon approaching $\eta = 0.8$ the jump in $\mathrm{Im}\Delta\chi_0(\mathbf{q}, \Omega_c^{(1)})$ decreases as $\mathbf{k}$ and $\mathbf{k}'$ approach the nodal points. Accordingly, the resonance frequency Ω_{res} moves closer to $\Omega_c^{(1)}$, and the intensity of the resonance decreases [5].

At $\mathbf{Q}_0 = 0.8(\pi, \pi)$, $\mathrm{Im}\chi_0(\mathbf{Q}_0, \Omega)$ is nonzero for all $\Omega > 0$ [see Fig. 4(c)]. At small frequencies, $\mathrm{Im}\chi(\mathbf{Q}_0, \Omega) = \gamma_{\mathbf{Q}_0}^{SC}\Omega$, where $\gamma_{\mathbf{Q}_0}^{\mathrm{SC}} = (1/8)\gamma_{\mathbf{Q}}^{NS}(\pi v_F/4v_\Delta)$ and v_Δ is the gap velocity at the nodal points. The factor $1/8$ arises since only a single (direct) scattering channel contributes to $\gamma_{\mathbf{Q}_0}^{\mathrm{SC}}$, while eight channels contribute to $\gamma_{\mathbf{Q}}^{NS}$. However, since the Fermi velocities at the nodal points are antiparallel, $\gamma_{\mathbf{Q}_0}^{\mathrm{SC}}$ depends on v_F only through the ratio $v_F/v_\Delta \sim 20$ which compensates the small prefactor. As a result, $\gamma_{\mathbf{Q}_0}^{\mathrm{SC}}$ is comparable to $\gamma_{\mathbf{Q}}^{NS}$, and $\mathrm{Im}\chi(\mathbf{Q}_0, \Omega)$ becomes similar to that in the normal state. The vanishing of the gap in the p-h continuum at $\mathbf{Q}_0$ together with the large value of $\gamma_{\mathbf{Q}_0}^{\mathrm{SC}}$ implies that at $\mathbf{q} = \mathbf{Q}_0$ the resonance completely disappears. This explains the experimental observation of a silent band in Ref. [7].

At the same time, $\mathrm{Re}\chi_0$ diverges logarithmically at $\Omega_c^{(2)}$, and hence it satisfies the resonance condition $\mathrm{Re}\Delta\chi_0(\mathbf{q}, \bar{\Omega}_{\mathrm{res}}) = \xi_{\mathbf{q}}^{-2}/g_{\mathbf{q}}$, at some frequency $\bar{\Omega}_{\mathrm{res}}$ below $\Omega_c^{(2)}$. At $\mathbf{q} = \mathbf{Q}_0$, this resonance is completely eliminated by damping. However, for momenta $\mathbf{q} < \mathbf{Q}_0$, (i.e., $\eta < 0.8$) the nodal points cannot be connected, and a *direct* gap opens for excitations into the p-h continuum. This gap is independent of the SC gap, and is given by $\Omega_c^d = \mathbf{v}_F \cdot (\mathbf{Q}_0 - \mathbf{q})$ [dashed-dotted line in Fig. 3(b)]. Because of a large $|\mathbf{v}_F|$, Ω_c^d becomes equal to $\bar{\Omega}_{\mathrm{res}}$ already close to $\mathbf{Q}_0$, at $q \approx 0.97Q_0$ for the dispersion of Eq. (2). Once Ω_c^d crosses $\bar{\Omega}_{\mathrm{res}}$, the damping at $\bar{\Omega}_{\mathrm{res}}$ vanishes and a true pole in $\mathrm{Im}\chi$ reemerges, leading to the appearance of the Q^* mode. [See Fig. 4(d) and open circles in Fig. 3(b).] Away from $\mathbf{Q}_0$ the Q^* resonance is rapidly suppressed. This suppression arises from the decrease of $\Omega_c^{(2)}$ and that of the bare static spin susceptibility, $\chi_0(\mathbf{q}, 0)$ at $q < Q_0$. Both effects lead to a rapid shift of the Q^* mode towards the edge of the p-h continuum, and to a decrease in its intensity. As a result, this resonance is only visible near $\mathbf{Q}_0$. We emphasize that only one resonance mode is present at any η: for $0.8 < \eta < 1$, it is the Q mode, for $\eta < 0.8$ it is the Q^* mode. This does not preclude that at a given $\mathbf{q}$, there exists a second, weaker peak in $\mathrm{Im}\chi(\omega)$ at higher frequencies (see Fig. 2). However, this second peak does not arise from a pole.

The Q and Q^* modes are not only separated in frequency, as discussed above, but their intensity maxima are also located in different parts of the zone; this represents a major qualitative distinction between the two modes. In Fig. 5 we present our numerical results for the intensity plots of $\mathrm{Im}\chi$ as a function of momentum for $\Omega > \Omega_{\mathrm{res}}(\mathbf{Q})$, probing the Q^* mode [Fig. 5(b)], and for $\Omega < \Omega_{\mathrm{res}}(\mathbf{Q})$, probing the Q mode [Fig. 5(a)]. The difference is striking. While the intensity of the Q mode is largest along $\mathbf{q} = (\pi, \eta\pi)$ and $\mathbf{q} = (\eta\pi, \pi)$, the Q^* mode has its largest intensity along the diagonal direction, i.e., along $\mathbf{q} = \eta(\pi, \pi)$ and $\mathbf{q} = [(2 - \eta)\pi, \eta\pi]$. This effect has also been obtained theoretically in Ref. [16].

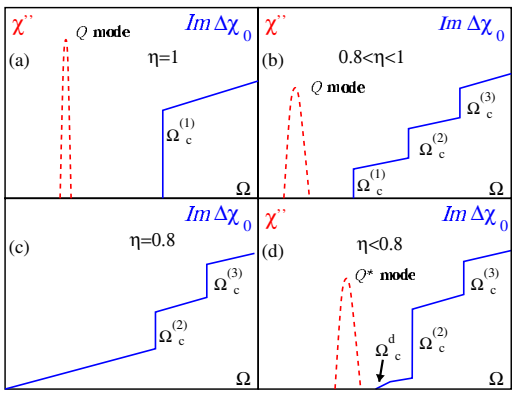

FIG. 4 (color online). Schematic behavior of $\mathrm{Im}\Delta\chi_0(q, \Omega)$ and $\mathrm{Im}\chi(q, \Omega)$ for $q = \eta(\pi, \pi)$. As η deviates from 1, the jump in $\mathrm{Im}\Delta\chi_0(q, \Omega)$ splits into three jumps at $\Omega_c^{(i)}$. At $\eta = 0.8$, $\Omega_c^{(1)} = 0$. At $\eta < 0.8$, a direct gap, Ω_c^d, opens.

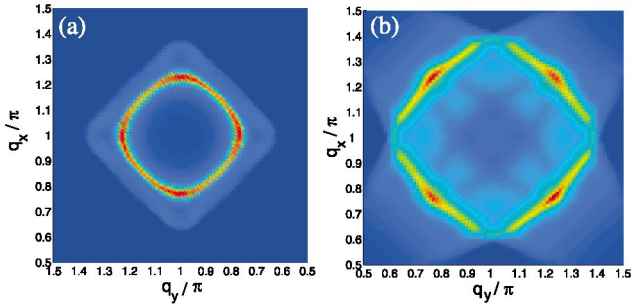

FIG. 5 (color). Intensity plot of $\mathrm{Im}\chi$, Eq. (1), as a function of momentum [blue (red)] implies a small (large) value of $\mathrm{Im}\chi$) at: (a) 30 meV (Q mode), and (b) 57 meV (Q^* mode). The Q mode forms a distorted ring in momentum space, with intensity maxima along (π, q). In contrast, the intensity of the Q^* mode is largest along the zone diagonal. In (b), the periodic structure of $\mathrm{Im}\chi$ around $\mathbf{Q}$ reflects the momentum dependence of the p-h continuum at this energy. The ratio of the maximum intensities along the diagonal and bond directions is 0.83 in (a) and 2.67 in (b).

This rotation of the intensity pattern by 45° reflects the qualitative difference in the origin of the two modes. The intensity of the Q mode is at a maximum along $\mathbf{q} = (\pi, \eta\pi)$ and $\mathbf{q} = (\eta\pi, \pi)$, since in this case the fermions that are scattered by $\mathbf{q}$ are located farther from the nodes than for diagonal scattering. In contrast, the Q^* mode arises from the rapid opening of a gap in the p-h continuum below $\mathbf{Q}_0$, which is most pronounced along the diagonal directions of the zone. We found that the intensity pattern of the Q^* mode remains diagonal in the whole range of frequencies where the Q^* mode exists, except very near the edge of the p-h continuum, where the pattern becomes bond centered for a narrow range of energies. This occurs because the p-h continuum edge is at a higher energy along the bond direction than along the diagonal. The diagonal pattern of the Q^* mode was observed in underdoped YBCO [8] while in optimally doped YBCO, the maximum intensity of the Q^* mode is along the bond directions [7]. Our own studies have shown that the orientation of the Q^* pattern at higher energies is sensitive to details of the particle-hole continuum.

In summary, we showed that a new resonant magnetic excitation at incommensurate momenta, observed recently by inelastic neutron scattering experiments on $YBa_2Cu_3O_{6.85}$ [7] and $YBa_2Cu_3O_{6.6}$ [8], is a spin exciton arising from umklapp scattering. Its location in the zone and its frequency are determined by the momentum dependence of the p-h continuum and reflects the Fermi surface topology. It is confined to a small region in $\mathbf{q}$ just below $\mathbf{Q}_0$, and is separated from the Q resonance by a silent band where $\mathrm{Im}\chi$ is strongly suppressed. We also found that the intensity maxima of the two modes are rotated by 45° relative to each other.

The issue left for further studies is the evolution of the new resonance in the underdoped cuprates. In our analysis with parameters representative of optimal doping, we found an upper cutoff of the Q^* mode at about 60 meV. Experimentally, the upper edge of the Q^* resonance increases with underdoping up to 100 meV in $YBa_2Cu_3O_{6.6}$, while the frequency Ω_{res} of the Q mode at (π, π) decreases [8]. This trend is consistent with the exciton scenario as the upper cutoff for the Q^* mode scales with the pairing gap, which increases with underdoping, while Ω_{res} is determined by ξ_Q^{-1}, which decreases with underdoping. Nevertheless, to properly treat the underdoped case and the evolution towards nonsuperconducting systems, such as $La_{1.85}Ba_{0.125}CuO_4$ [17], will require taking into account the pseudogap and Mott physics. Note in this regard that the RPA reproduces the observed spin waves in the undoped material only if the Mott gap is taken into account [18].

We thank Ph. Bourges, S. Hayden, B. Keimer, and H. Mook for discussions concerning their data. I. E. is thankful to INTAS (No. 01-0654) and RSP Superconductivity Grant No. 98014-3 for support. D. K. M. acknowledges support from the Alexander von Humboldt foundation. A. C. acknowledges support from NSF DMR 0240238 and SFB 290. M. R. N. is supported by the US Department of Energy, Office of Science, under Contract No. W-31-109-ENG-38. D. K. M. and A. C. are grateful for the hospitality of the Freie Universität Berlin. D. K. M., A. C., and M. R. N. also acknowledge support from the Aspen Center for Physics where this work was completed.

*On leave from the Physics Department, Kazan State University, 420008, Kazan, Russia.

[1] J. Rossat-Mignod *et al.*, Physica C (Amsterdam) **185**, 86 (1991); H. F. Fong *et al.*, Phys. Rev. B **61**, 14773 (2000); P. Dai, H. A. Mook, R. D. Hunt, and F. Dogan, Phys. Rev. B **63**, 054525 (2001).
[2] H. F. Fong *et al.*, Nature (London) **398**, 588 (1999).
[3] H. He *et al.*, Science **295**, 1045 (2002).
[4] H.-Y. Kee, S. A. Kivelson, and G. Aeppli, Phys. Rev. Lett. **88**, 257002 (2002); Ar. Abanov *et al.*, Phys. Rev. Lett. **89**, 177002 (2002).
[5] H. F. Fong *et al.*, Phys. Rev. Lett. **75**, 316 (1995); Ar. Abanov and A. V. Chubukov, Phys. Rev. Lett. **83**, 1652 (1999); J. Brinckmann and P. A. Lee, Phys. Rev. Lett. **82**, 2915 (1999); Y.-J. Kao *et al.*, Phys. Rev. B **61**, R11 898 (2000); F. Onufrieva and P. Pfeuty, Phys. Rev. B **65**, 054515 (2002); D. Manske, I. Eremin, and K. H. Bennemann, Phys. Rev. B **63**, 054517 (2001); M. R. Norman, Phys. Rev. B **61**, 14751 (2000); **63**, 092509 (2001); A. Chubukov, B. Janko, and O. Tchernyshov, Phys. Rev. B **63**, 180507(R) (2001).
[6] L. Yin, S. Chakravarty, and P. W. Anderson, Phys. Rev. Lett. **78**, 3559 (1997); E. Demler and S. C. Zhang, Phys. Rev. Lett. **75**, 4126 (1995); D. K. Morr and D. Pines, Phys. Rev. Lett. **81**, 1086 (1998); M. Vojta and T. Ulbricht, Phys. Rev. Lett. **93**, 127002 (2004); G. S. Uhrig, K. P. Schmidt, and M. Gruninger, Phys. Rev. Lett. **93**, 267003 (2004); C. D. Batista, G. Ortiz, and A. V. Balatsky, Phys. Rev. B **64**, 172508 (2001).
[7] S. Pailhes *et al.*, Phys. Rev. Lett. **93**, 167001 (2004).
[8] S. M. Hayden *et al.*, Nature (London) **429**, 531 (2004).
[9] D. Reznik *et al.*, Phys. Rev. Lett. **93**, 207003 (2004).
[10] The well known limitations of the RPA approach suggest that corrections beyond RPA might become relevant at higher energies of order J.
[11] For the numerical calculation of χ_0, we used $i\omega_n \rightarrow \omega + i\delta$ with $\delta = 2$ meV.
[12] A. Damascelli, Z. Hussain, and Z.-X. Shen, Rev. Mod. Phys. **75**, 473 (2003).
[13] This expression is valid for interacting fermions as long as the fermionic self-energy does not depend on the momentum transverse to the Fermi surface.
[14] $\mathrm{Re}\Delta\chi_0 \neq 0$ only if one includes the curvature of the dispersion in the normal state.
[15] D. K. Morr and D. Pines, Phys. Rev. B **62**, 15177 (2000); **61**, R6483 (2000).
[16] A. P. Schnyder *et al.*, Phys. Rev. B **70**, 214511 (2004).
[17] J. M. Tranquada *et al.*, Nature (London) **429**, 534 (2004).
[18] J. R. Schrieffer, X. G. Wen, and S. C. Zhang, Phys. Rev. B **39**, 11663 (1989).